Analyses of Instability in Mobile Cranes due to Ground Penetration by Outriggers

Satoshi Tamate[1]; Naoaki Suemasa[2]; and Toshiyuki Katada[3]

Abstract: This study focuses on the phenomenon of ground instability causing mobile cranes to overturn. Four outriggers usually support a mobile crane in order to restrict pitching during hoisting operations. Nevertheless, the crane may become quite unstable if the outriggers should happen to sink into the bearing ground. In this paper, various types of analysis, including experiments, were performed in order to investigate the influence of ground penetration by outriggers on the stability of mobile cranes. Through study of the results of experimentation and simulation, it has been clarified that mobile cranes become highly unstable as a result of rapid penetration. It was found that an index of relative instability had a linear relationship to the common logarithm of an index for brittle failure as derived from the load–settlement curve for ground penetration. Finally, a method of evaluating the risk of mobile-crane overturning is proposed by using the maximum value of both the supporting surface's failure risk and the kinetic risk due to ground penetration.

DOI: 10.1061/(ASCE)0733-9364(2005)131:6(689)

CE Database subject headings: Cranes; Stability; Bearing capacity; Brittle failure; Centrifuge model; Numerical analysis; Safety analysis.

Introduction

Mobile cranes are comprised of hoisting machinery combined with both a base carrier and a revolving superstructure. These cranes, either mounted directly onto wheels or truck mounted, usually stand on four outriggers that are located at the corners of the lower base carrier. The outriggers extend laterally and bear on the ground during hoisting operations to keep the crane horizontal. Many accidents have occurred due to overturning of such mobile cranes, and the number of casualties reaches approximately 100 each year in Japan (Japan Crane Association 2002); further, it is also considered that the same problem would exist in countries throughout the world.

Several research projects aimed at the prevention of overturning have been undertaken with a focus on the dynamic forces caused by the action of wind and by structural vibration of the crane itself. Zaretsky and Shapiro (1997) introduced a simplified dynamic analysis method that was simulated using an equivalent linear system. Beliveau et al. (1993) mentioned the necessity of damping out payload oscillations during crane operation and also proposed a control system comprising a yoke around the load hoist cable so that increases in tipping moment could be prevented. Bernold et al. (1997) developed an intelligent monitoring system that prevented deviation from safe loading conditions. In these projects, however, the crane foundation was assumed to be either elastic or sufficiently stiff.

Rajagopalan (1988) described a case history that referred to foundation design in the setting up of mobile cranes on a sloped site, and in addition, indicated countermeasures using pile foundations. The bearing capacity of ground required to ensure the stability of mobile cranes has not been standardized from geotechnical research.

Ground penetration by outriggers was observed in many cases where actual overturning occurred (see Fig. 1). In addition, about 20% of overturning incidents occurred when the hook load was less than the net rated load prescribed by safety regulations. The forces acting through the outriggers can be estimated as 70–80% of the sum of the machinery weight and the hook load (Ito 1994). Although safety regulations for mobile cranes worldwide prescribe the net rated load as a limitation of the maximum permitted hook load, the ground is assumed to be sufficiently hard and firm (U.S. Department of Labor, Occupational Safety and Health Administration 1994; Standards Association of Australia 1993a,b; British Standards Institution 1991a,b, 2000; International Organization for Standardization 1991; Japan Crane Association 1998). The necessary ground conditions for setting up mobile cranes are not specifically prescribed in regulations. Further, the influence of both depth of ground penetration and sinking behavior on overturning is also not considered. Despite improvements in the mechanical safety of machinery, many overturning accidents still occur. Accordingly, safety can only be ensured by taking the ground condition into consideration during evaluation of the risk of overturning.

[1]Senior Researcher, Construction Safety Research Group, National Institute of Industrial Safety (NIIS), 1-4-6 Umezono, Kiyose, Tokyo 204-0024, Japan.

[2]Associate Professor, Dept. of Civil Engineering, Faculty of Engineering, Musashi Institute of Technology, 1-28-1 Tamazutsumi, Setagaya-ku, Tokyo 158-8557, Japan.

[3]Professor, Dept. of Civil Engineering, Faculty of Engineering, Musashi Institute of Technology, 1-28-1 Tamazutsumi, Setagaya-ku, Tokyo 158-8557, Japan.

Note. Discussion open until November 1, 2005. Separate discussions must be submitted for individual papers. To extend the closing date by one month, a written request must be filed with the ASCE Managing Editor. The manuscript for this paper was submitted for review and possible publication on August 26, 2003; approved on June 28, 2004. This paper is part of the ***Journal of Construction Engineering and Management***, Vol. 131, No. 6, June 1, 2005. ©ASCE, ISSN 0733-9364/2005/6-689–704/$25.00.

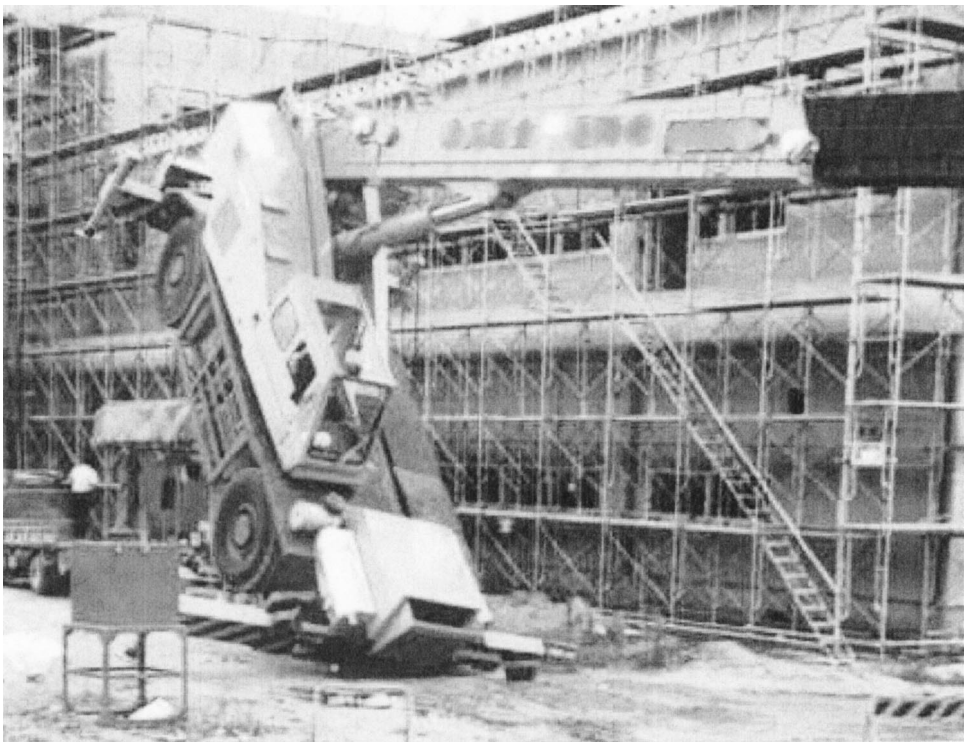

Fig. 1. Overturning of a mobile crane due to ground penetration by the outriggers

It is thought that instability in the ground—and in particular, the probability of brittle failure—is an underlying cause in many overturning accidents. To prevent these accidents, it is important to clarify the relationship between overturning and ground penetration by the outriggers. This study focuses on ground penetration by outriggers and the resulting overturning of mobile cranes.

Theoretical Instability of Mobile Cranes

It is assumed that mobile cranes become unstable due to ground penetration of outriggers through two types of mechanism—namely, static instability and kinetic instability. When the outriggers penetrate the ground gradually and the machinery tilts slowly, moment increases due to the hook load's lever arm becoming longer as a result of rotation of the jib (ΔR in Fig. 2). This problem is applicable to the stability of a jack-up rig on the seabed. Ingram and Dutt (1987) and Hambly (1985, 1990) indicated the necessity of considering the increasing overturning moment due to the tilt, regardless of the increase in strength due to the penetration of the leading footing in the seabed. In addition, mobile cranes are set up on ground of varying conditions, and this may fail suddenly and lead to rapid penetration of outriggers. Kinetic instability is caused by an increase in gyration energy as a result of the angular velocity of the mobile crane, and in addition to the static instability, this is also an important factor for consideration. Static equilibrium and dynamic equilibrium are summarized in this section.

Static Equilibrium

Static equilibrium was calculated with the assumption that ground penetration by the outriggers occurs at a negligibly slow speed. Consequently, the static equilibrium occurs at the maximum tilt angle where the crane is perfectly balanced while hoisting the hook load. When the outrigger at the fulcrum penetrates the ground, the lever-arm length increases due to tilting of the crane. A formula for static equilibrium is derived in the following equation for cases where the mobile crane is set up on a flat ground surface:

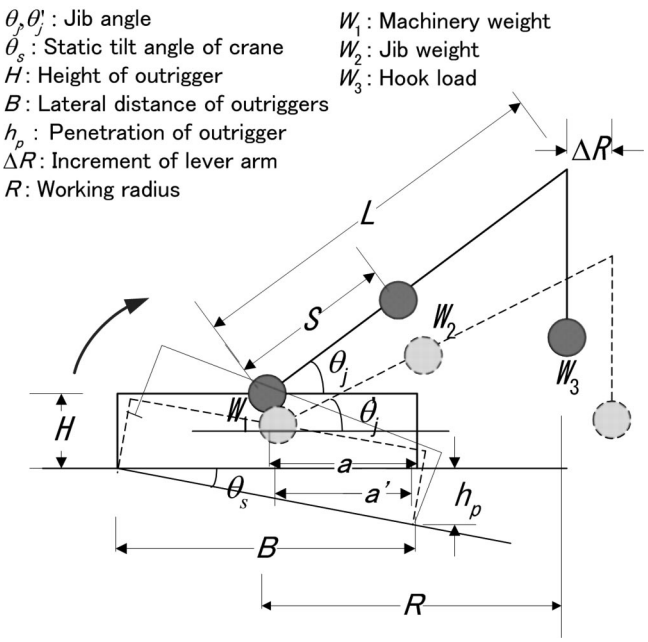

Fig. 2. Schematic view of overturning due to penetration by the outriggers

J. Constr. Eng. Manage., 2005, 131(6): 689-704

Table 1. Comparison of Safety Factors for Hook Load in the Stability of Mobile Cranes Supported by Outriggers

USA[a]	United Kingdom[b]	Australia[c]	ISO[d]	Japan[e]
1.17(=1/0.85)	1.25	1.33(=1/0.75)	1.25	1.27

[a]U.S. Department of Labor, Occupational Safety and Health Administration, 2000.

[b]British Standards Institution, 1991.

[c]Standards Association of Australia, 1995.

[d]International Organization for Standardization, 1991.

[e]Labour Standard Bureau, Ministry of Labour, Japan, 1978.

$$W_1 a = W_2(S\cos\theta_j - a) + W_3(L\cos\theta_j - a) \quad (1)$$

where W_1=machinery weight; W_2=jib weight; W_3=critical hook load at the static equilibrium; θ_j=jib angle; L=jib length; S=length between the jib's fulcrum and center of gravity; and a=lateral distance between the center of gravity of the whole crane (G) and the outrigger at the overturning fulcrum. These iterations are explained in Fig. 2. The net rated load is calculated by dividing W_3 by the safety factor as prescribed in the safety regulations: This factor ranges between 1.17 and 1.33 in global regulations (see Table 1) where the ground surface is assumed to be both level and sufficiently hard and firm.

The static tilt angle of the crane (θ_s) is defined using the point at which the crane reaches static equilibrium. θ_s refers to the ratio of the critical depth of ground penetration by the outrigger (h_p) to the lateral distance between the outriggers (B), and θ_s is thus expressed as

$$\theta_s = \sin^{-1}(h_P/B) \quad (2)$$

Further, the jib angle with respect to the ground surface (θ_j') is expressed as shown in

$$\theta_j' = \theta_j - \theta_s \quad (3)$$

The lateral distance (a') between the center of gravity (G) and the front outrigger reduces due to crane tilt, and this is calculated as

$$a' = (B/2)\cos\theta_s - H\sin\theta_s \quad (4)$$

The following equation represents static equilibrium when ground penetration of the outriggers is taken into account, and here, W_3' is a critical hook load upon crane tilt (θ_s)

$$W_1 a' = W_2(S\cos\theta_j' - a') + W_3'(L\cos\theta_j' - a') \quad (5)$$

Dynamic Equilibrium

Dynamic equilibrium was derived under the assumption that ground penetration by the outriggers occurs rapidly. In addition, its velocity was assumed to be the same as that for free fall (Maeda and Inoue 1985). The schema for dynamic overturning is shown in Fig. 3, and the decrease in potential energy due to ground penetration by the outriggers is fully converted into gyration energy about the overturning fulcrum. Accordingly, dynamic overturning was assumed to occur when the accumulated gyration energy exceeds the remaining work against gravity [i.e., when the center of gravity (G) raises by a height (Δh_2) and moves above the fulcrum of overturning]. The dynamic equilibrium corresponds to the maximum tilt angle at which the crane could balance when hoisting the hook load if the fulcrum were to fall freely to the depth of outrigger ground penetration.

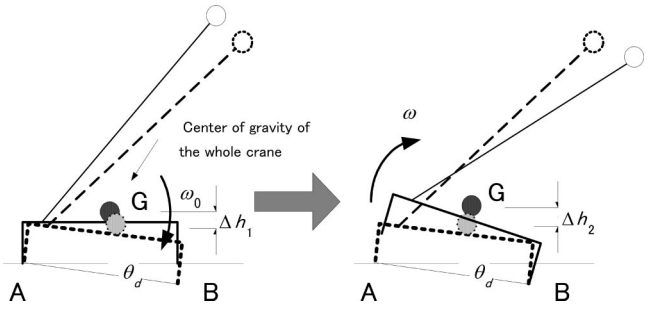

Fig. 3. Dynamic overturning due to rapid penetration

The relationship between angular velocities ω and ω_0 (in Fig. 3) is derived in following equation for a situation where the fulcrum is shifted from the rear outriggers to the front outriggers:

$$\omega = (k^2 + r^2 - ab)\omega_0/(k^2 + r^2) \quad (6)$$

where k=radius of rotation and r, a, and b=parameters shown in Fig. 4.

Further, ω and ω_0 are defined by application of the law of energy conservation in

$$\omega_0^2 = 2g\Delta h_1/(k^2 + s^2) \quad (7)$$

$$\omega^2 = 2g\Delta h_2/(k^2 + r^2) \quad (8)$$

where Δh_1 indicates the vertical downward displacement of the center of gravity (G) as a result of tilting around the rear outriggers and Δh_2 indicates the vertical upward displacement around the front outriggers.

The relationship between Δh_1 and Δh_2 is defined in by substituting Eqs. (7) and (8) into Eq. (6) as in

$$\Delta h_2 = c\Delta h_1 \quad (9)$$

where

$$c = (k^2 + r^2 - ab)^2/((k^2 + r^2)(k^2 + s^2)) \quad (10)$$

Δh_1 and Δh_2 are expressed in the following equations for mobile crane geometry as shown in Fig. 4:

$$\Delta h_1 = h - h\cos\theta_d + (B - a)\sin\theta_d \quad (11)$$

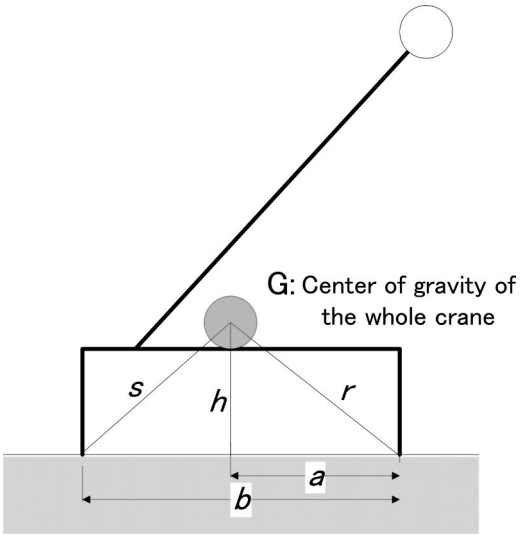

Fig. 4. Geometric parameters for calculation of dynamic equilibrium

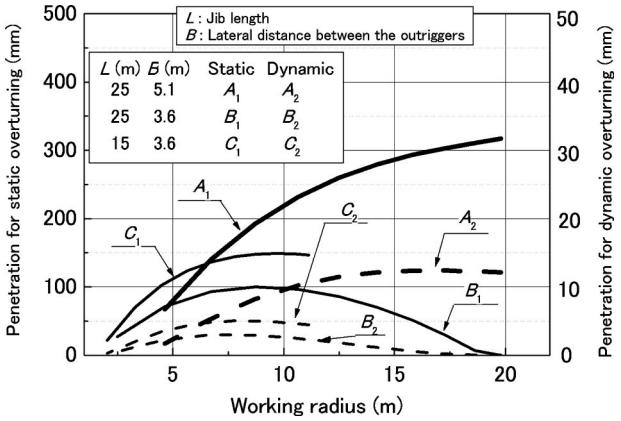

Fig. 5. Comparison between static and dynamic equilibrium for the prototype crane

$$\Delta h_2 = r - h\cos\theta_d - a\sin\theta_d \tag{12}$$

Here, the dynamic tilt angle θ_d is defined as the point at which the crane reaches dynamic equilibrium, and this is derived as shown in the following equation by substituting Eqs. (11) and (12) into Eq. (9):

$$\sin\theta_d = (V - \sqrt{V^2 - UW})/U \tag{13}$$

where

$$U = \{(c-1)a - bc\}^2 + h^2(c-1)^2 \tag{14}$$

$$V = (ch - r)\{(c-1)a - bc\} \tag{15}$$

$$W = (r-h)(r - 2ch + h) \tag{16}$$

The critical depth of ground penetration by the outrigger (h_d) as caused by reaching dynamic equilibrium is derived as

$$h_d = B\sin\theta_d \tag{17}$$

Fig. 5 shows both the relationship between the critical depth of ground penetration by the outriggers with regard to overturning and the working radius (R in Fig. 1) (Tamate et al. 1998a). R is the projected length of the jib onto the horizontal plane as represented by the ground. The solid lines and dotted lines show the critical depths for static equilibrium and dynamic equilibrium respectively for a prototype wheel crane with a 200 kN hoisting capacity. This result shows the influence of both the crane's working condition and the velocity at ground penetration on overturning. Parameters for the working condition comprise both the jib length (L) and the lateral distance between outriggers (B), where the hook load is equivalent to the net rated load at the working radius. A safety factor of 1.27 was adopted in calculation of the net rated load (Japan Crane Association 1998). The curve A_1 shows the critical depth at the static equilibrium, and this depth becomes larger with increases in the working radius when $L=25$ and $B=5.1$. It is determined that the crane becomes unstable in an area with a small working radius and with a higher jib angle at the static equilibrium, even though the hook load is equivalent to the net rated load. The critical depth at the dynamic equilibrium (A_2) represents a smaller value than that of A_1 over the entire working radius, and consequently, the mobile crane becomes highly unstable as a result of rapid penetration. It has also been confirmed that the working condition of the mobile crane affects the critical depth. The critical depths for both static equilibrium (B_1) and dynamic equilibrium (B_2) when $L=25$ and $B=3.6$ m become smaller than those of A_1 and A_2, respectively. This indicates that a narrower lateral distance between the outriggers induces a lower stability in mobile cranes: The crane can hardly bear even a small amount of rapid penetration. It is thus confirmed that the stability of a mobile crane depends on the ground-penetrating behavior of the outriggers as a result of bearing-ground failure, as well as on the working conditions of mobile crane itself.

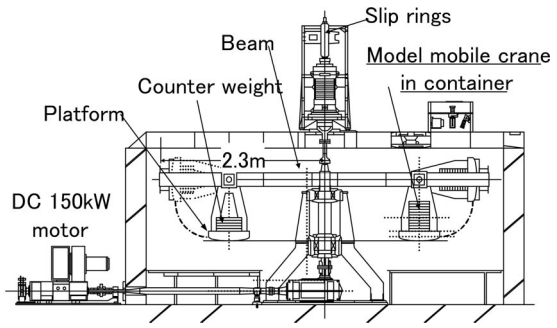

Fig. 6. Schematic view of the NIIS geotechnical centrifuge

Centrifuge Test for Simulation of Overturning

Experimental Apparatus

Simulation of overturning using a mobile-crane model was performed in order to investigate the instability in such a crane as caused by ground penetration by outriggers following failure of the supporting surface. The mobile-crane model used in the experiment (Tamate et al. 1998b) was a 1/20-scale prototype wheel crane with a hoisting capacity of 200 kN. Simulation of overturning was carried out using a National Institute of Industrial Safety (NIIS) geo-technical centrifuge (see Fig. 6) in such a way that the pressure acting through the crane model's outriggers was equivalent to that of the prototype mobile crane. Fig. 7 shows the testing apparatus used for simulated overturning in a centrifuge test.

The model crane simulates overturning caused by reducing the jib angle, thereby lengthening the hook load's lever arm and the moment. This provides an effective means of investigating the relationship between outrigger ground penetration and overturning, and it realistically simulates not only overturning for various types of ground condition, but also the mobile crane's moment.

The crane model consists of both a lower base and an upper crane unit. A pair of outrigger beams (No. 1 in Fig. 7) is attached to both ends of a base plate (No. 2) which is made from aluminum alloy; further, this plate has a width of 100 mm, a length of 200 mm, and a thickness of 15 mm. A pair of outriggers (No. 3) is fixed vertically to each end of the outrigger beams, and the model stands on four outriggers positioned at the body corners. Circular-shaped outrigger floats (or footings, No. 5) are set under the outriggers to distribute the pressure evenly over the ground surface, and the diameter of each float is 30 mm. A small load cell (No. 4) and a wire-type displacement meter (No. 17) are installed on all outriggers to measure the relationship between load and settlement.

The upper crane mechanism principally consists of a mechanical device to decrease the jib angle in the centrifuge, and an ac servomotor is used to provide motive power (No. 6). The jib angle is reduced by rotating a screw gear (No. 8) using several

J. Constr. Eng. Manage., 2005, 131(6): 689-704

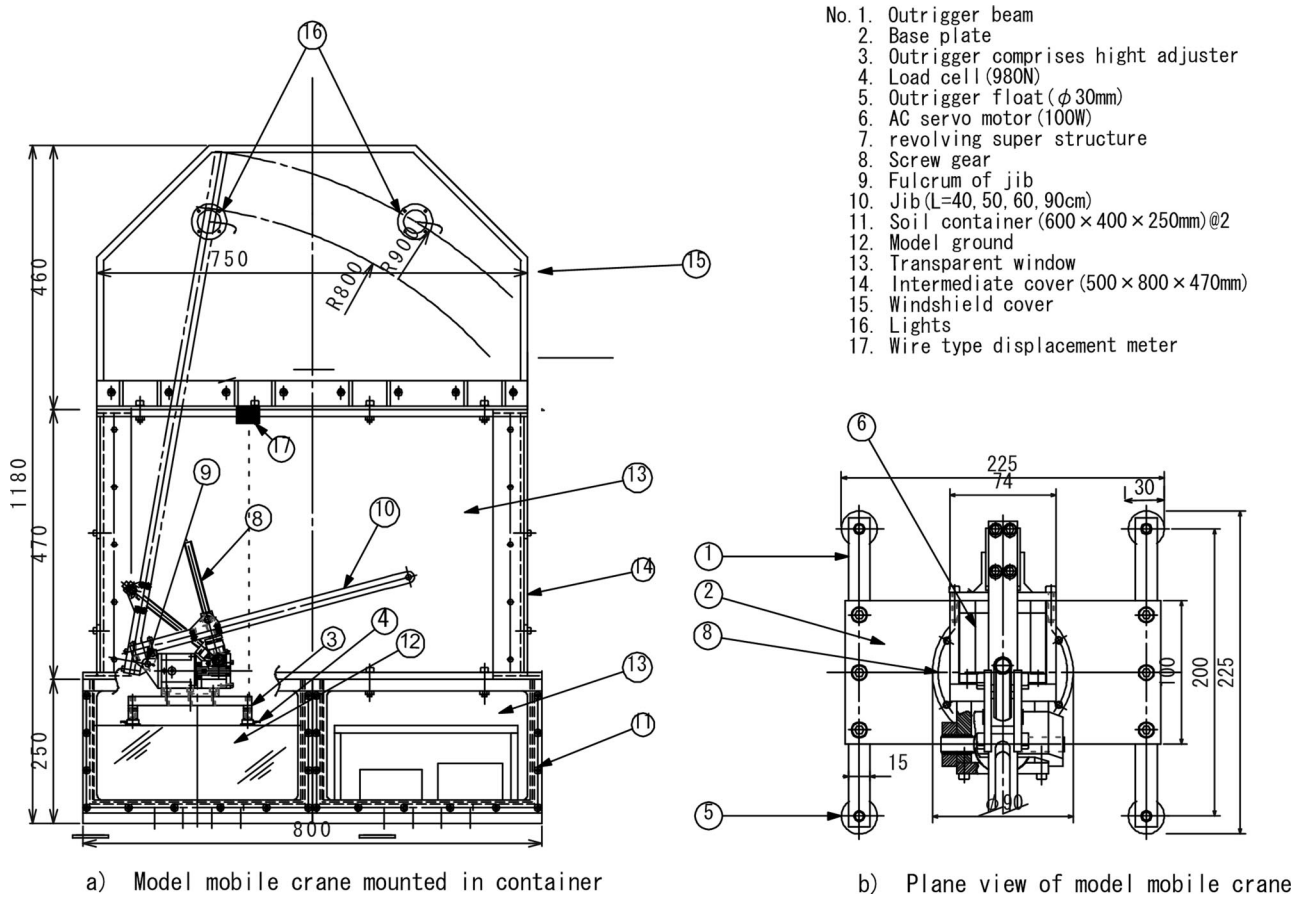

Fig. 7. Model mobile crane in container for simulation of overturning by centrifuge; (a) Model mobile crane mounted in container and (b) Plane view of model mobile crane

other gears connected to the servomotor. The fulcrum of the jib (No. 9) is located at the back of the motor, and the jib angle varies between 15 and 75° with respect to the lower base.

A testing container with high sides was used to prevent the effect of strong wind due to centrifuge rotation during the tests.

Model Ground

Mobile cranes are used on bearing ground of a wide range of different conditions, and unsaturated soil is considered to be the normal ground condition for the setting up of mobile cranes. Accordingly, the tests were performed using two types of model ground to induce different ground penetration characteristics, and these types were:

1. Uniform, soft loam, and
2. Layered ground with a hard surface covering soft soil.

The soil used in the tests was Kanto loam—a volcanic, cohesive soil found in Japan—and this soil was deposited to form the model ground. Table 2 lists the physical properties of this soil. Kanto loam was filtered through a sieve with a 2 mm mesh and sprayed with water prior to use in order to provide conditions of optimum moisture content. The linear relationship between the pressure at static compression (p_c) and the unconfined compressive strength (q_u) was found by conducting unconfined compression tests. The rate of strength increase (q_u/p_c) was 0.426 for $p_c < 147$ kPa.

Table 2. Properties of Kanto-loam

Specific gravity	2.72
Liquid limit (%)	120.7
Plastic limit (%)	82.4
Plastic index	38.3
Optimum moisture content (%)	85
Strength increasing ratio q_u/p	0.426

A loam–cement mixture was produced by mixing an ultrarapid hardening cement with the loam so as to simulate a hard surface for the model ground. Loam was placed inside a strong container in order to make uniform ground, and statically compressed with a loading plate and a bellofram cylinder at 147 kPa. The hard surface formed from the loam–cement mixture was cast directly onto the uniform ground to produce a layered structure. The mixture ratio of cement to loam was chosen such that the unconfined compressive strength of the loam–cement mixture (q_{ud}) would be equivalent to the dried and hardened loam on site. The thicknesses of the hard surfaces (H) were set to 15, 30, and 42 mm to give $H/D = 0.5$, 1.0, and 1.8, respectively, relative to the diameter of the float (D). The total thickness of the ground was 150 mm.

Centrifuge Test Procedure

Two sets of test conditions for the mobile-crane model were established prior to the centrifuge test. One set comprised working conditions such as the lateral distance between the outriggers and the jib length, whereas the other corresponded to the moment

J. Constr. Eng. Manage., 2005, 131(6): 689-704

Table 3. Test Conditions and Results of Simulation

Name of tests	CT1	CT2	CT3	CT4[a]	CT5	CT6[b]	CT7	CT8	CT9
Condition of ground[c]	Uniform Soft ground	Layered	Layered	Layered	Layered	Layered	Layered	Layered	Layered
Thickness of hard surface (H)/ diameter of the float (D)	0	0.5	1.0	1.0	1.0	1.0	1.0	1.0	1.8
Unconfined compressive strength of loam-cement mixture (kPa), q_{ud}	—	598	598	598	598	598	598	598	264
Centrifugal acceleration (g)	17	38	49	45	52	72	52	72	52
Jib length (mm), L	600	600	600	400	600	900	600	900	600
Hook load (N)	9.6	9.6	9.6	25.0	9.6	3.1	14.6	5.5	9.6
Tipping jib angle without penetration (deg), ϕ_a	30	30	30	30	30	30	45	45	30
Jib angle at overturning (deg), ϕ_b	37.5	44.0	46.5	56.2	54.0	60.5	60	57	53
Tilt angle of crane at interpreted equilibrium (deg), θ_a	1.3	5.2	5.2	—	8.0	—	5.9	—	10.8
Tilt angle of crane at static limiting equilibrium (deg), θ_s	1.9	6.2	7.3	11.0	10.8	17.3	8.8	9.8	10.2
Tilt angle of crane at dynamic limiting equilibrium (deg), θ_d	0.1	0.4	0.6	1.5	1.4	3.5	1.0	1.1	1.2
Tilt angle of crane at kinetic equilibrium (deg), θ_r	1.2	4.9	3.1	6.6	4.8	7.0	3.8	4.7	8.9
Index of instability, $I_r = \sin\theta_r / \sin\theta_s$	0.63	0.79	0.42	0.60	0.44	0.39	0.43	0.48	0.86
Tilt angle of crane at analytical equilibrium (deg), θ_N	2.1	5.2	3.8	5.1	4.8	7.5	3.9	4.5	6.8
Analytical index of instability, $I_{rN} = \sin\theta_N / \sin\theta_s$	1.10	0.83	0.52	0.45	0.44	0.42	0.44	0.45	0.66

[a]Broken outrigger during the overturning disturbed the movement of overturning.

[b]Overturning stopped due to the jib touching the container wall.

[c]Layered=hard surface overlying on the uniform soft ground.

condition governed by the relationship between the jib angle and the hook load. The tipping jib angle (ϕ_a) refers to the minimum angle of the jib hooking the load without any ground penetration by the outriggers. The jib angle at overturning (ϕ_b) is defined in consideration of ground penetration during the centrifuge test.

The pressure acting through all outriggers was maintained at a constant level as the jib angle was kept higher, and this was chosen as the initial condition prior to testing. The moment was increased by reducing the jib angle at constant centrifugal acceleration. One of the aims of the test was to investigate the mechanism of overturning caused by ground penetration by the outriggers even when the mobile crane itself continued to maintain the condition of static stability achieved prior to reaching static equilibrium.

The pressure acting through the outriggers was controlled using a combination of centrifugal acceleration and the mass of the model including the hook load. Variations in centrifugal acceleration do not affect the moment; accordingly, the stability of the mobile crane in the centrifuge was equivalent to that of the prototype. Consequently, the centrifuge acceleration was varied so as to give different pressures acting through the outriggers for identical values of moment. The model ground's yield stress was studied using bearing capacity tests prior to the centrifuge testing so as to determine the acceleration of the centrifuge. Both the conditions and results for the centrifuge test are listed in Table 3. Fig. 8 presents an overview of the testing apparatus used in the simulation of overturning. It was observed that the crane model overturned due to ground penetration by the outriggers, even though the jib made contact with the wall of the container.

Experimental Analysis of Model Tests

Characteristics of Bearing Capacity and Model Ground Penetration

Fig. 9 shows the relationship between the acting pressure (q) and normalized ground penetration by the front outriggers (s/D) in the testing of three different types of model ground. The acting pressure q was calculated by dividing the outrigger's acting load by the area of the outrigger float. s/D refers to the ratio of ground penetration by the front outrigger (s) to the diameter of the outrigger float (D). Since CT1 for the uniform ground bent at a q value of approximately 147 kPa, the ground's yield pressure was almost equivalent to the pressure at static compression (p_c). The ratio s/D for CT1 increases rapidly when q rises above p_c; further, the curves for both CT2 and CT3 show results for layered ground, and H/D for these are 0.5 and 1.0, respectively, when $q_{ud}=600$ kPa for the surface. Both curves show that the ground's bearing capacity increases in proportion to the thickness of the harder surface.

Differences in the postyield behavior of ground penetration can be seen in the three ground types. Although q does not increase after yielding in CT3 and the curve shows a tendency to be flat, a clear increase can be seen in CT1. The postyield response for CT2 shows an intermediate tendency for q to increase between CT1 and CT3. The postyield behavior of outrigger penetration depends on the status of the hard surface overlaying the lower base ground. It was also observed that the velocity of ground penetration shown in CT3 ($H/D=1.0$) is the highest of all

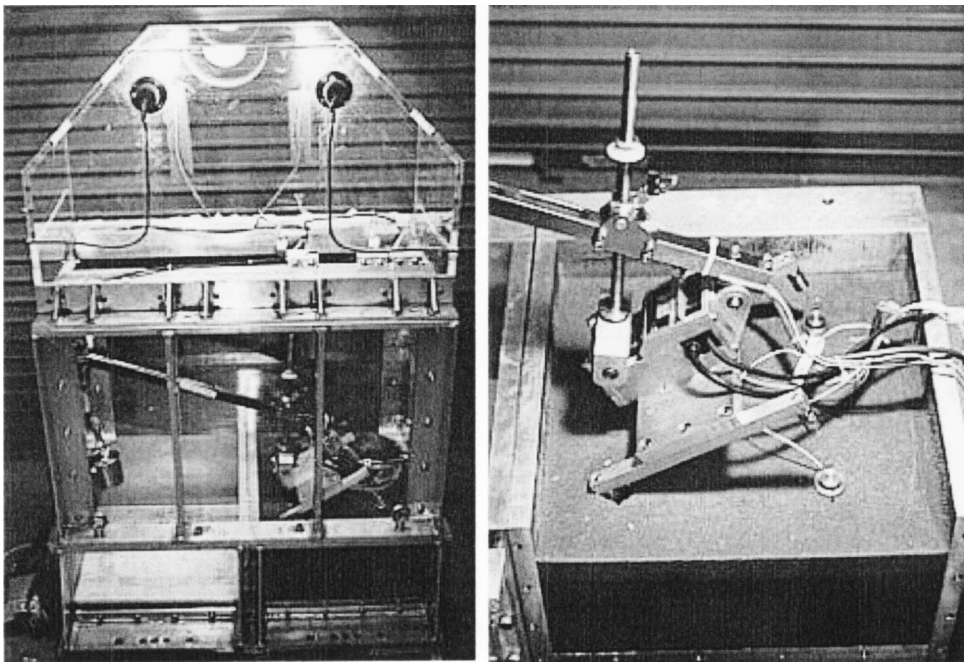

Fig. 8. Model mobile crane in container for centrifuge test (left) and ground penetration by the outriggers (right)

three. Finnie (1993) also referred to the risk of the overturning of a jack-up rig that is set up on a seabed. The bearing capacity tests for a shallow foundation were carried out on the layered model ground, and this comprised a hard layer of cement mixture overlaying silt ground with a normal consolidation. The resistance to footing penetration reduced after peaking at the point where the footing punched through the upper thin layer. Consequently, rapid penetration in this type of layered ground increases the risk of overturning as a result of the gyration energy produced in the mobile crane and in the jack-up rig.

Fig. 10 shows the relationship between q and s/D for both the front outrigger and the rear outrigger during the test. The front outrigger acted as the fulcrum of overturning, and following this, the rear outrigger acted as the fulcrum of crane tilting prior to overturning. The two curves are almost identical up to about 1,000 kPa due to an increase of the centrifugal acceleration (see the two circles in Fig. 10), and this implies that the pressure acting through the outriggers was almost equivalent at the front and rear as the jib angle was kept higher. After reaching the predetermined level of centrifugal acceleration as shown in Table 3, q for the front outriggers increased as the jib angle decreased, and s/D increased sharply once the pressure exceeded about 1,200 kPa. By contrast, q for the rear outriggers reduced from 1,000 to 0 kPa. The interpreted equilibrium is defined at the zero reaction for the rear outrigger, and in addition, the tilt angle of the crane at the interpreted equilibrium is also defined as the interpreted tilt angle (θ_a).

Fig. 11 shows a section profile of the model ground at outrigger penetration (CT2). The model ground comprised 15 mm of an upper hard layer made from a cement–loam mixture overlaying a lower base of loam. The outrigger penetrated about 40 mm into the model ground, and cylindrical failure and several slip lines can be seen in the upper layer. Since no upward swelling was observed at the ground surface, it would indicate that punching occurred due to failure.

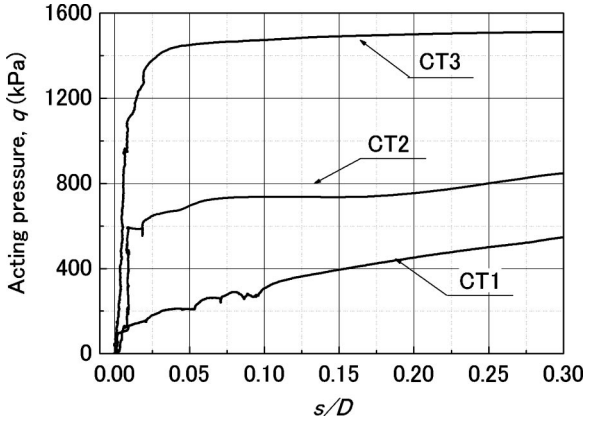

Fig. 9. Comparison of bearing characteristics of three types of model ground

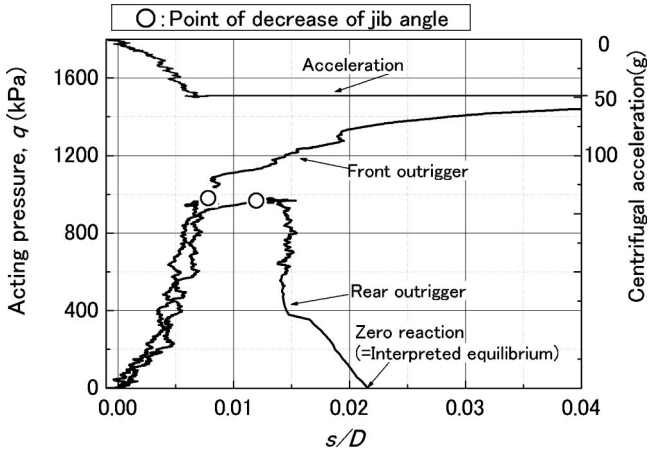

Fig. 10. Relationship between acting pressure (q) and s/D in the centrifuge testing ($H/D=1$, CT3)

J. Constr. Eng. Manage., 2005, 131(6): 689-704

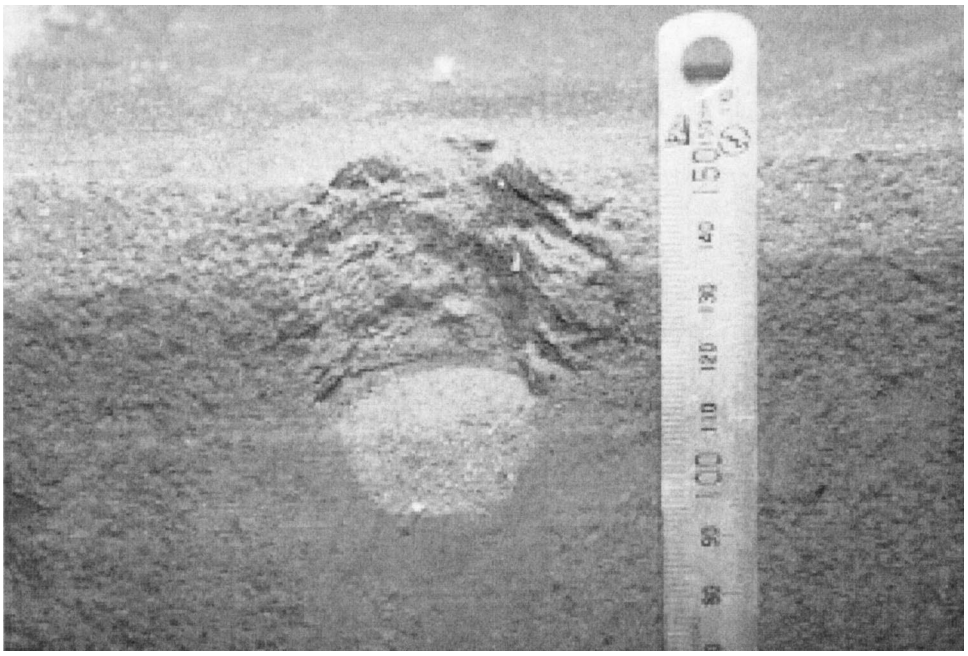

Fig. 11. Section profile for ground penetration by the outrigger (CT2)

Experimental Analysis

Interpreted Equilibrium

Fig. 12 shows the relationship between the tilt angle of the crane and the jib angle. The tilt angle of the crane was calculated by dividing the differential settlement (Δs) between the front and rear outriggers by the lateral distance between the outriggers, and this is shown on the vertical axis. The jib angle and elapsed time for the tests are shown on the lower and upper horizontal axes, respectively. The jib angle reduced from 75° at constant centrifugal acceleration, and triangles indicate the interpreted tilt angle (θ_a) in each case. Both the static equilibrium and the dynamic equilibrium are also indicated by dotted lines. The model crane in CT1 tilted linearly with a decrease of the jib angle and θ_a was marked at 1.3°. The tilting increment remained almost constant at 0.1°/s. When the jib angle reached about 55° in CT2, the tilt angle increased at a high rate of approximately 17 times that for CT1. It was determined that the cranes for both CT1 and CT2 overturned upon reaching the static equilibrium as the corresponding θ_a were located just under this point. Meanwhile, when the jib angle reached about 47° in CT3, rapid penetration occurred as a result of brittle failure of the ground, and the crane overturned quickly with a θ_a of 5.8°, located under static equilibrium and close to dynamic equilibrium. This result indicates that the crane became unstable before reaching the static equilibrium. Rapid penetration of the outriggers made the crane much more unstable.

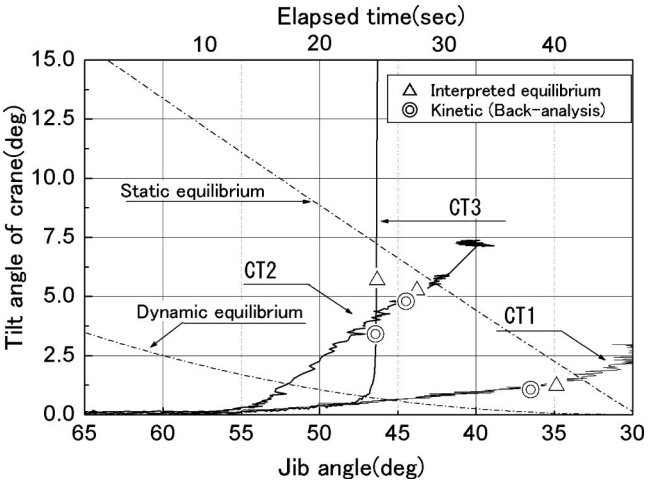

Fig. 12. Relationship between tilt angle of the crane and jib angle at overturning

Kinetic Equilibrium—Backanalysis

Kinetic equilibrium was derived from the test record for ground penetration by the outriggers. The gyration energy that results from crane tilting about the rear outriggers (i.e., fulcrum *A* from Fig. 3) due to ground penetration by the front outriggers transfers fully to gyration energy about the front outriggers. The angular velocity (ω_0) around *A* is calculated using the test record of ground penetration by the front outriggers (i.e., point *B* from Fig. 3). Second, the angular velocity (ω) around *B* is calculated under the assumption that the gyration energy about fulcrum *A* was converted into gyration energy about fulcrum *B*. The relationship between ω_0 and ω was introduced in Eq. (6) in the preceding section. Third, the increment in the energy due to gravity (Δh_a), or in other words, the vertical displacement of the center of gravity (*G*) caused by the rapid penetration, is calculated as

J. Constr. Eng. Manage., 2005, 131(6): 689-704

Table 4. Tilt Angle of Crane at Equilibriums

Titles of the tilt angles	Conditions
Static tilt angle (θ_s)	Theoretical limitation of static equilibrium in consideration of the outrigger penetration
Dynamic tilt angle (θ_d)	Theoretical limitation of dynamic equilibrium where the outrigger penetrates rapidly and its speed is assumed as same as that at free fall
Interpreted tilt angle (θ_a)	Experimental result at zero reaction of the backward outrigger
Kinetic tilt angle (θ_r)	Experimental result of dynamic equilibrium calculated by back-analysis using of the test record

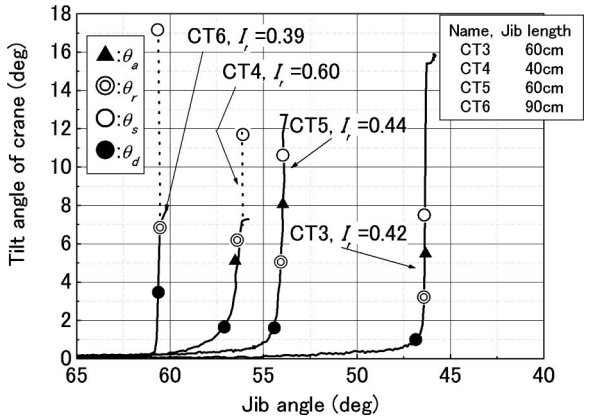

Fig. 13. Influence of jib length (L) and jib angle at the overturning (ϕ_b) on the index of relative instability (I_r)

$$\Delta h_a = \frac{(k^2 + r^2)\omega^2}{2g} \tag{18}$$

Meanwhile, the necessary vertical displacement (Δh_b) for overturning is determined by the condition of the crane, and this is derived in

$$\Delta h_b = r - h\cos\theta_0 - a\sin\theta_0 \tag{19}$$

where θ_0=crane's tilt angle.

Consequently, overturning as a result of reaching kinetic equilibrium occurs when

$$\Delta h_a > \Delta h_b \tag{20}$$

is satisfied. The crane's kinetic tilt angle (θ_r) is defined as the point at which the crane reaches the kinetic equilibrium. Explanations for each tilt angle are summarized in Table 4.

θ_r is indicated by a double circle in Fig. 12, and θ_r for both CT1 and CT2 is located near the corresponding θ_a. This result shows that a slight amount of gyration was present as a result of the lower velocity of ground penetration in both cases, and this is also confirmed by θ_r moving closer to static equilibrium. Accordingly, this type of the overturning is categorized as static overturning.

Meanwhile, θ_r was smaller than θ_a in CT3 and was positioned in the intermediate area between the static and dynamic equilibriums. The reason for this was that the velocity of penetration for CT3 was higher than that for both CT1 and CT2. Rapid penetration of the front outriggers (i.e., fulcrum *B* in Fig. 3) induced higher angular velocity about the rear outriggers, and the crane subsequently reached kinetic equilibrium prior to reaching the zero reaction of the rear outriggers. This type of overturning is categorized as dynamic overturning. However, θ_r was larger than the dynamic equilibrium, and the reason for this was that the actual velocity of outrigger penetration was lower than that of free fall. It is considered that the existence of shear resistance in the ground reduced the velocity of penetration. Consequently, it was clarified that θ_s and θ_d indicate the upper and the lower equilibrium, respectively. The actual equilibrium (θ_r) exists between θ_s and θ_d, and this varies in accordance with the penetration velocity; further, this velocity also depends on the failure characteristics of the ground.

Fig. 13 shows the relationship between the tilt angle of the crane and the jib angle during overturning for CT3, CT4, CT5, and CT6, and the influence of jib angle and jib length (L) on overturning will be considered first. The ground condition for these cases corresponded to a hard surface overlaid on soft ground. The relative thickness of the hard layer (H/D) was 1.0, and its unconfined compressive strength (q_{ud}) was adjusted to 600 kPa so as to simulate rapid penetration by outriggers due to the brittle failure of the ground. Although the same length of jib was given for the crane in both CT3 and CT5, the jib angle at overturning (ϕ_b) was different in each case, and this indicates that the moment at overturning was also different. One aim of comparing ϕ_b was to investigate the influence of the given moment for the crane on overturning. Quick tilting of the crane was seen for ϕ_b=46.5° in CT3, and in this case, both θ_a and θ_r existed between θ_s and θ_d. Moreover, dynamic overturning occurred as mentioned above since θ_r was smaller than θ_a. Meanwhile, ϕ_b =54.0° for CT5, and here the difference between CT3 and CT5 was 7.5°. Accordingly, the moment at overturning for CT3 was larger than that for CT5, and consequently, θ_a, θ_r, θ_s, and θ_d for CT3 were smaller than those for CT5.

The potential for initial instability prior to ground penetration by the outriggers is affected by the given moment. A relative index is needed to enable evaluation of the influence of ground penetration by the outriggers on overturning where variations exist in the potential for instability. The potential for initial instability can be expressed as θ_s, and the instability due to ground penetration by the outriggers is expressed as θ_r. Thus, an index for relative instability (I_r) which takes θ_s and θ_r into account is defined as

$$I_r = \frac{\sin\theta_r}{\sin\theta_s} \tag{21}$$

I_r values for the test results are listed in Table 3, and these are generally distributed between 0 and 1. A lower value of I_r indicates that the crane overturned quickly due to rapid penetration.

L=600 mm for CT3 and CT5, and the corresponding I_r values were calculated at 0.42 and 0.44, respectively. Although L =900 mm for CT6, I_r was calculated as 0.39, and this value is almost the same as that of the previous cases. I_r for CT4 was calculated at 0.6—a higher value than that of the above cases—and the reason for this was that late failure in test CT4 occurred due to a broken outrigger, and this resulted in the higher value of I_r. Thus, it was found that differences in both jib length and jib angle at overturning have little effect on the relative instability of the crane.

J. Constr. Eng. Manage., 2005, 131(6): 689-704

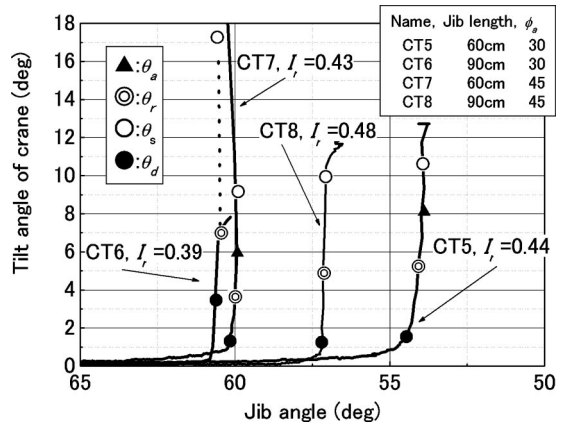

Fig. 14. Influence of L and tipping jib angle (ϕ_a) on I_r

Fig 14 shows the results for CT5, CT6, CT7, and CT8, and the influence of the jib length (L) and the tipping jib angle (ϕ_a) on I_r is presented. ϕ_a is the tipping jib angle of a crane that overturns without outrigger penetration. Differences in hook load gave an individual tipping jib angle (ϕ_a) of 30 and 45° in CT5 and CT7, respectively, and the jib length was identical at 600 mm. ϕ_a values of 30 and 45° were given for CT6 and CT8, respectively, and these had a 900 mm value for L. Changing the combination of ϕ_a and L varies the weight balance of the crane. In actuality, θ_r was distributed over a wide range; however, I_r was almost identical in the range 0.39–0.48. It was confirmed, therefore, the differences in L and ϕ_a do not have much effect on I_r.

Fig 15 shows the results for CT2, CT5, and CT9, and the influence of the outrigger's penetration characteristics on I_r is presented. Although the crane had identical conditions where L =600 mm and ϕ_a=30° in each of these cases, the corresponding ground conditions were different. The relative thickness of the surface layer (H/D) was 0.5 in CT2; 1.0 in CT5; and 1.8 in CT9. An unconfined compressive strength (q_d) of 600 kPa was given for the surface layer of both CT2 and CT5, and a q_{ud} value of 260 kPa was given for CT9. The combination of thickness (H) and strength (q_{ud}) for the hard surface was chosen so as to simulate various velocities of ground penetration by the outriggers. Moreover, the ground's yield stress was almost identical between CT5 (H/D=1, q_d=600 kPa) and CT9 (H/D=1.8, q_d=260 kPa).

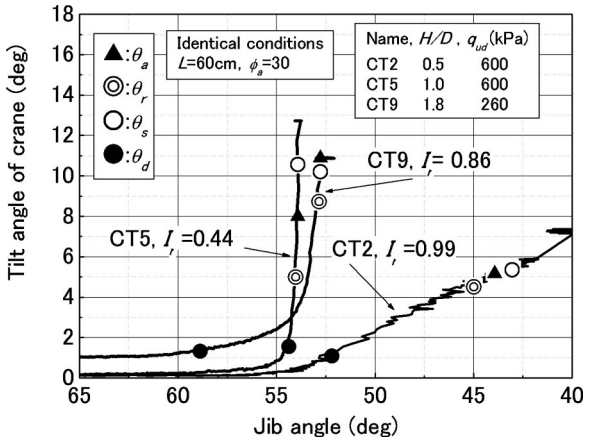

Fig. 15. Influence of difference of characteristics of ground penetration on I_r

Brittle failure of the ground induced rapid penetration of the outrigger in CT5, and a value of 0.44 was then indicated for I_r—this being the smallest of all three cases. Meanwhile, slow penetration due to ductile failure was observed in both CT2 and CT9, and this resulted in I_r values of 0.79 and 0.86, respectively.

It was clear from experimental analysis that the velocity of ground penetration by the outriggers affected I_r, even though this was affected very little with regard to the stability of a mobile crane by differences in both the working condition and the moment. Consequently, it is important to evaluate the risk of the overturning not only in terms of the bearing capacity of the ground, but also with regard to the characteristics of ground penetration caused by brittle failure of the bearing ground.

Numerical Calculation for Overturning

Numerical calculation was carried out to verify the test results and to clarify the influence that characteristics of ground penetration have on instability. The method used for the calculation is described in this section.

Calculating the Time History for Overturning

The equation of motion is then obtained as shown in the following equation when the damping force induced by the dispersion energy at ground penetration is considered:

$$[M]\frac{d^2u}{dt^2} + [C]\frac{du}{dt} + [K]u + \{R\} = 0 \tag{22}$$

where M=matrix of the inertia mass; C=matrix of the damping factor; K=matrix of the tangent modulus of the subgrade ground reaction; R=matrix of the moment of overturning; and u=tilt angle of the crane.

The time history for overturning of the crane as a result of ground penetration by an outrigger was calculated using Newmark's method (Cook et al. 1989), where this was adapted to the equation of motion. A direct integration using this method enabled the prediction of motion in the time domain.

Numerical calculation was carried out to simulate the centrifuge test procedure for overturning as shown in Fig. 16. (1) The jib angle is reduced to increase the moment of overturning; (2) the crane tilts due to outrigger penetration; and (3) this then leads to overturning. It can be determined that large deformation occurs because of the decrease in both jib angle and crane tilt. Consequently, the problem of nonlinearity due to large deformation must be taken into account in the calculation.

Nonlinearity problems are usually solved by separation into a series of linear steps. The instantaneous coefficients $[M]$, $[C]$, $[K]$, and $[R]$ from the equation of motion are written in the current configuration, and the equation of motion at an arbitrary time t_i is presented in

$$[M_i]\ddot{u}(t_i) + [C_i]\dot{u}(t_i) + [K_i]u(t_i) + \{R_i\} = 0 \tag{23}$$

where i=calculation time step.

The equation of motion at $t+\Delta t$ is presented in the following equation, and variables for the angular acceleration, the angular velocity, and the tilt are calculated using Newmark's method:

$$[M_i]\ddot{u}(t_i + \Delta t) + [C_i]\dot{u}(t_i + \Delta t) + [K_i]u(t_i + \Delta t) + \{R_i\} = 0 \tag{24}$$

J. Constr. Eng. Manage., 2005, 131(6): 689-704

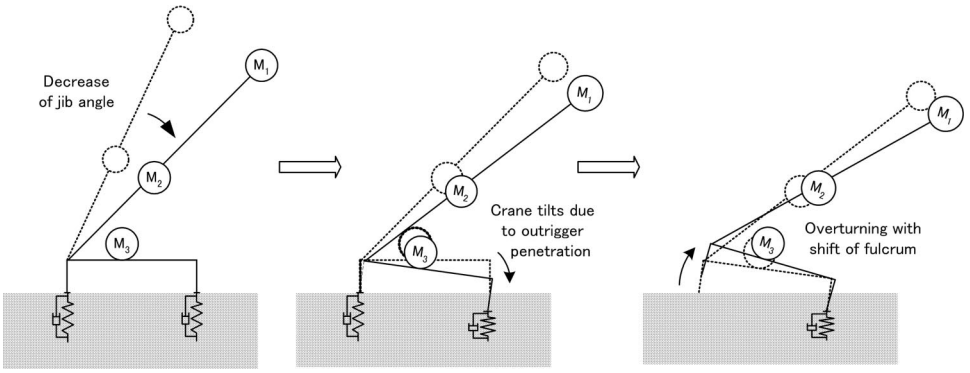

Fig. 16. Procedure of overturning for simulation by numerical calculation

Ground penetration induces an increase in moment due to the ground″s elastic strain energy ($\Delta\{R\}$), where this is the product of an increment in ground penetration (i.e., $u(t_i+\Delta t)-u(t_i)$) and $[K_i]$. $\Delta\{R\}$ is given by

$$\Delta\{\mathbf{R}\} = [K_i] \times (\mathbf{u}(t_i + \Delta t) - \mathbf{u}(t_i)) \tag{25}$$

In consideration of the new configuration, coefficients for the current shape must be updated at every step of the calculation. The time $(t_i+\Delta t)$ from Eq. (24) is replaced with the time t_{i+1}. The increment $\Delta\{R\}$ occurring during Δt is repeatedly added to the moment in accordance with the subgrade reaction of the ground. Thus, the updated equation of motion is given as

$$[M_{i+1}]\ddot{u}(t_{i+1}) + [C_{i+1}]\dot{u}(t_{i+1}) + [K_{i+1}]u(t_{i+1}) + \{R_{i+1}\} = 0 \tag{26}$$

in which

$$t_{i+1} = t_i + \Delta t \tag{27}$$

$$\{R_{i+1}\} = \{R_i\} + \Delta\{R\} \tag{28}$$

The tilt angle and the angular velocity at t_{i+1} are replaced for the subsequent calculation of overturning as shown in

$$u(t_{i+1}) = 0 \tag{29}$$

$$\dot{u}(t_{i+1}) = \dot{u}(t_i + \Delta t) \tag{30}$$

However, a problem due to discontinuity exists in Eq. (26), and the reason for this is that both the coefficients and the variables are updated at the same time in the new configuration. Thus, $\ddot{u}(t_{i+1}) \neq \ddot{u}(t_i+\Delta t)$ leads to an error in calculation, and therefore, this problem due to discontinuity was solved by modifying the angular acceleration as obtained by

$$\ddot{u}(t_{i+1})_{\text{mod}} = \frac{-\{R_{i+1}\} - [C_{i+1}]\dot{u}(t_{i+1}) - [K_{i+1}]u(t_{i+1})}{[M_{i+1}]} \tag{31}$$

The equation of motion used for the updated calculation is given by

$$[M_{i+1}]\ddot{u}(t_{i+1})_{\text{mod}} + [C_{i+1}]\dot{u}(t_{i+1}) + [K_{i+1}]u(t_{i+1}) + \{R_{i+1}\} = 0 \tag{32}$$

The time history for overturning is calculated by repeated implementation of this procedure.

Condition of Calculation

Calculation Models

Numerical calculation of overturning was performed using two-dimensional models. The procedure for calculation is as follows: First, the gravitational acceleration was increased to the same level as the acceleration for the centrifugal test so as to simulate overturning at equivalent conditions. Next, the jib angle was reduced to increase the moment, and finally, calculation was completed by reaching either kinetic equilibrium or static equilibrium.

The fulcrum of rotation was assumed to be positioned at the rear outriggers at the start of tilting. This fulcrum was shifted from the back to the front when the reaction at the rear outrigger reduced to zero, and then variables for the tilt angle, the angular velocity, and the angular acceleration were recalculated for the front outrigger in consideration of the preservation of kinetic energy during rotation. All of the coefficients were also required to be calculated for the front outrigger.

Relationship between Acting Pressure and Ground Penetration by Outriggers

Two types of the model for the relationship between the acting pressure (q) and ground penetration by outriggers (s/D) were used in the numerical calculation. The hyperbola model as presented in the following equation was used to verify both CT1 and CT9, and the corresponding relationships between acting pressure and penetration are shown as curves in accordance with ductile failure of the ground:

$$q = \begin{cases} \dfrac{1}{\dfrac{1}{\varepsilon n_1 K_0} + \dfrac{1}{n_2 q_{\max}}} & \text{(virgin loading)} \\ n_1 K_0 \varepsilon & \text{(unloading and reloading)} \end{cases} \tag{33}$$

where ε=ground penetration by outriggers normalized by the diameter of the outrigger (s/D); K_0=initial tangent modulus of the relationship between q and ε; $q_{\max}$=maximum pressure value for q; and both n_1 and n_2=arbitrary coefficients.

The bilinear model,

$$q = \begin{cases} n_3 K_0 \varepsilon & (q \leqslant q_y) \quad \text{(virgin loading)} \\ n_4 K_y(\varepsilon - \varepsilon_y) + q_y & (q \geqslant q_y) \quad \text{(virgin loading)} \\ n_3 K_0 \varepsilon & \text{(unloading and reloading)} \end{cases} \tag{34}$$

consists of a primary path folded at the yield pressure and connecting to a secondary path which corresponds to the previous

J. Constr. Eng. Manage., 2005, 131(6): 689-704

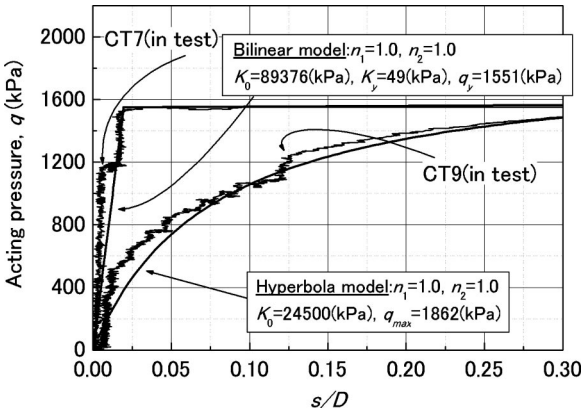

Fig. 17. Comparison of bearing characteristics of ground between test and approximation

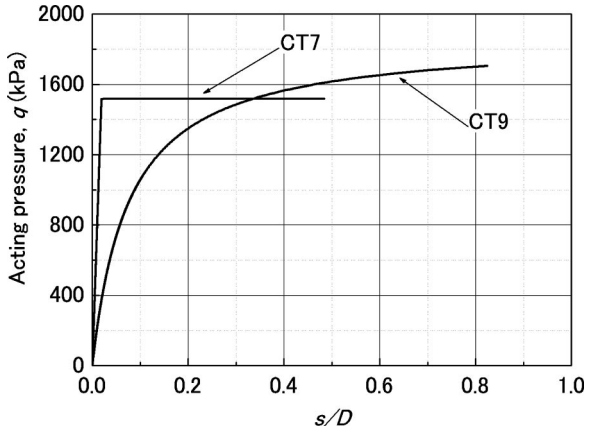

Fig. 18. Relationship between acting pressure (q) and s/D of front outrigger in numerical calculation (CT7 and CT9)

linear relation; further, this model was used to verify cases from CT2 to CT8 where the corresponding relationships exhibited winding due to brittle failure of the ground. In Eq. (34), ε_y = normalized settlement at the yield pressure; K_y = tangent modulus after yield; and both n_3 and n_4 = arbitrary coefficients.

Fig. 17 shows a comparison between the test results and modeled approximation results with respect to both CT7 and CT9. The bilinear model adhered to the test result for CT7, where rapid penetration occurred due to the brittle failure of the ground. In addition, the test result for CT9 showed a tendency for the tangent modulus to decrease with increases of ε, and q gradually settled at $q_{\max}$. The hyperbola model conformed well with the test result for CT9, where penetration occurred slowly due to ductile failure of the ground.

Damping Coefficient for Ground Penetration by Outriggers

Damping force caused by viscosity of the soil and slipping between soil particles affect the ground penetration by the outriggers. Accordingly, the damping force at overturning was calculated in consideration of the test record. An investigation of the relationship between the damping coefficient (C_i) and the tangent modulus for the ground reaction (K_i) was carried out for the centrifuge test settings. It was found that C_i was approximated to a K_i of 1/500, although differences were identified in this relationship. For the sake of simplicity, therefore, proportional damping of $C_i = K_i/500$ was adopted in the numerical calculation.

Numerical Parameters in Calculation

$\gamma = 1/2$ and $\beta = 1/4$ Newmark parameters were used in calculation so that the acceleration remained constant at an average acceleration between t and $t+\Delta t$. No numerical damping was used, and a time step Δt was required to be set to a small number to ensure accurate calculation. Accordingly, Δt was set to 1/60,000 s as calculated using 1/10th of the natural frequency of a crane standing on the ground. The jib angle was reduced at a constant speed of 1°/s to increase the overturning moment. It generally took approximately 10 minutes for calculation of overturning to perform 1.56×10^7 iterations using a 1.0 GHz personal computer.

Results of Calculation

Fig. 18 shows the relationship between the outriggers' acting pressure (q) and the normalized settlement (s/D) in the numerical calculation. The $q-s/D$ curves so obtained coincided with the given relationship shown in Fig 17, and it was ascertained that numerical calculation was correct. Iteration of the calculations for CT7 and CT9 stopped at 0.48 and 0.81 in each s/D because the crane reached either kinetic equilibrium or static equilibrium.

Fig. 19 shows an example of the time history for q corresponding to CT7 from the centrifuge test. Specifically, q for both the front outrigger and the rear outrigger increased with time although a small difference could be seen in these as a result of slight unbalance in the moment. Although the front q increased, the rear q reduced when the jib angle was decreased after 220 s of elapsed time. Calculation is completed when the front pressure reaches approximately 1,700 kPa. Meanwhile, 300 kPa of rear pressure remained at that time, and this indicates that the crane overturned prior to reaching static equilibrium. Therefore, numerical calculation enabled the simulation of overturning as a result of kinetic instability.

Fig. 20 compares the results of the relationship between the centrifuge test and numerical calculation. The analytical tilt angle (θ_N) is defined as a tilt angle at which the crane reached the analytical equilibrium—either static or the kinetic—in the numerical calculation. θ_N is marked by a square in Fig. 20 as well as being summarized in Table 3.

Correspondence in the behavior for overturning can be seen by comparing the curves for numerical calculation and for the cen-

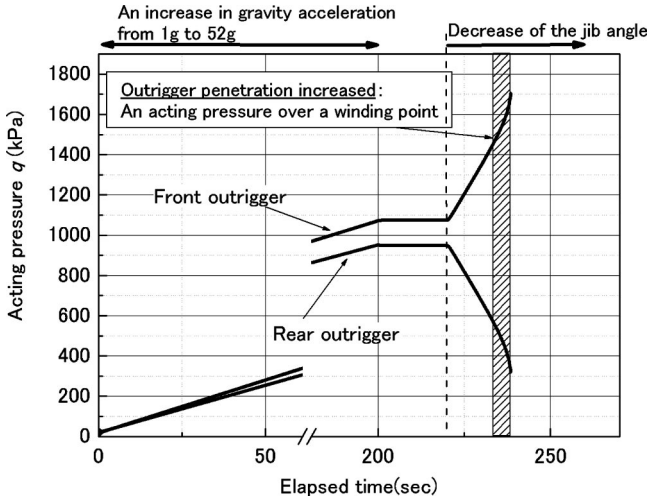

Fig. 19. Time history of acting pressure (q) in CT7

J. Constr. Eng. Manage., 2005, 131(6): 689-704

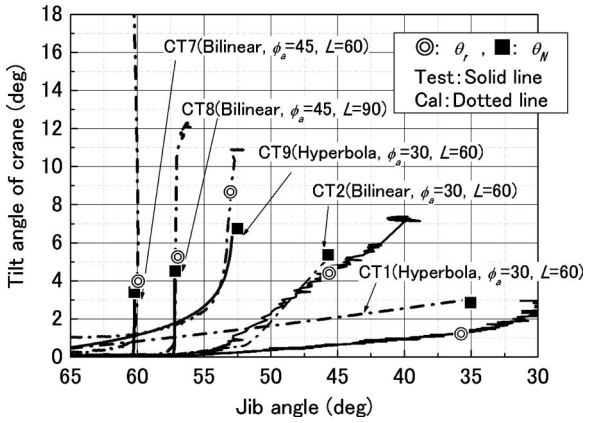

Fig. 20. Comparison of results between centrifuge test and numerical calculation

trifuge test. The behavior for overturning as obtained through numerical calculation generally coincided with the results from centrifuge tests in all cases except CT1. The reason for the difference between the test and the calculation in the case of CT1 may possibly be caused by both underestimation of the damping force and the slight difference in the relationship between q and s/D. Therefore, the tilt angle for the crane in numerical calculation was overestimated with respect to that from the centrifuge test, even when the jib angle was equivalent. Behavioral factors other than overturning as obtained using numerical calculation fitted well with the test, regardless of differences in ground condition, crane condition, and moment condition.

Correspondence of equilibrium can be seen in the comparison of θ_r and θ_N. Generally θ_N coincided with θ_r for CT2, CT7, and CT8, where a bilinear model was used for calculation so as to simulate brittle failure of the ground. Meanwhile, a difference was noticed between θ_N and θ_r for both CT1 and CT9. A hyperbola model was used for the calculation to simulate ductile failure of the ground. θ_N for CT9 was at least 2.1 degrees higher than θ_r, even though the behavior of overturning coincided between testing and calculation. Underestimation of the damping force in calculation also represented one of the reasons for this. The gyration energy of the mobile crane was overestimated in calculation, and the model reached kinetic equilibrium earlier than in the test. It was determined that the characteristics of the damping force at ground penetration must be clarified in order to achieve accurate calculation of the analytical equilibrium.

Risk Evaluation for Overturning with Regard to Ground Bearing Capacity and Penetration

Instability of the mobile crane as a result of ground penetration by outriggers and induced by failure of the bearing ground was discussed in the preceding section using the results of theoretical analysis, experimental analysis, and numerical analysis. Evaluation of the risk of overturning in consideration of ground condition is needed in order to prevent overturning prior to the setup of mobile cranes on the ground. The effect of both the bearing capacity of the ground and the characteristics of ground penetration by the outrigger upon overturning are discussed in this section.

Proposal for a Method of Risk Evaluation in Terms of Ground Conditions

The risk of overturning must be evaluated in terms of both of the following conditions: namely, the pressure acting against the yield pressure of the bearing ground and the characteristics of ground penetration by the outriggers. The failure risk for the bearing ground (r_p) is defined as the ratio of the acting pressure (q_a) to the ground's yield pressure (q_y), and this is shown in

$$r_p = \frac{q_a}{q_y} \tag{35}$$

The risk of overturning due to failure of the bearing ground increases when r_p is larger than 1. The maximum acting pressure during hoisting operations is expressed as q_a, and this is introduced either by analytical calculation which allows for the crane condition (i.e., hook load, crane weight, etc.) or by simple calculation as shown in

$$q_a = \frac{0.8(W_1 + W_2)}{A} \tag{36}$$

where W_1=weight of the crane; W_2=hook load; and A=area of the acting pressure.

The static risk due to ground penetration by the outriggers (r_s) is discussed next. The risk r_s is defined as the ratio of s_a to s_y as

$$r_s = \frac{s_a}{s_s} \tag{37}$$

where s_a=ground penetration induced by q_a and s_y=ground penetration at the static equilibrium for the mobile crane. The risk of overturning (D_{OT}) is defined as shown in the following equation, and the value of D_{OT} depends on the maximum values of both r_p and r_s:

$$D_{OT} = \max(r_p, r_s) \tag{38}$$

However, it was ascertained that kinetic overturning occurs when the mobile crane tilted rapidly due to brittle failure in the bearing ground. Accordingly, the kinetic risk (r_s') due to ground penetration is introduced to allow for ground penetration at the kinetic equilibrium (s_r). r_s' is

$$r_s' = \frac{s_a}{s_r} = \frac{r_s}{I_r} \tag{39}$$

and in this equation, I_r=index of the relative instability as mentioned previously. Consequently, r_s from Eq. (38) is replaced by r_s', and D_{OT} is modified as shown

$$D_{OT} = \max(r_p, r_s') \tag{40}$$

The relationship obtained by dividing r_p by r_s is described in the following equation where it is assumed that $r_s' > r_p$, $q_a < q_y$ and that q_a/s_a is equivalent to the initial tangent modulus (K_0) relationship between q and s:

$$\frac{r_p}{r_s} = \frac{q_a/q_y}{s_a/s_s} = K_0 \frac{s_s}{q_y} \tag{41}$$

Eq. (41) is substituted into Eq. (39), and then r_s' is derived as

$$r_s' = f r_p \tag{42}$$

Here, f is defined as

J. Constr. Eng. Manage., 2005, 131(6): 689-704

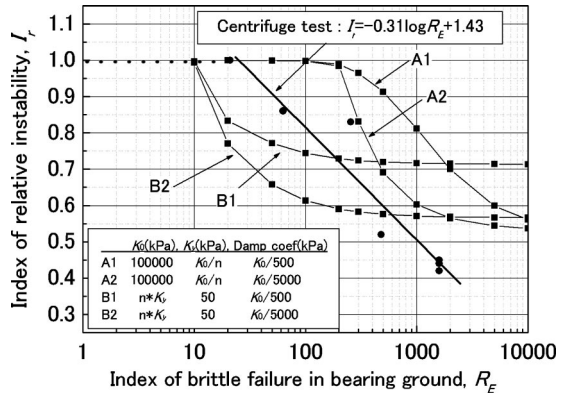

Fig. 21. Relationship between index of relative instability (I_r) and index of brittle failure in the bearing ground (R_E)

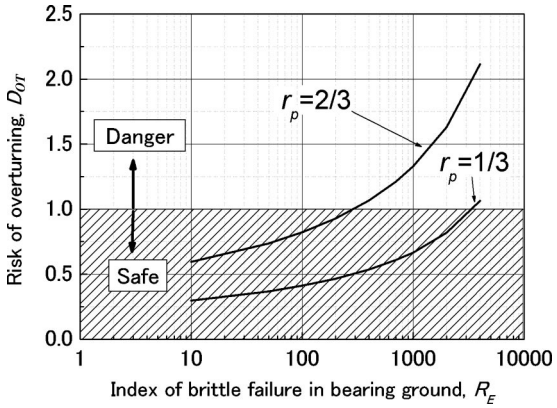

Fig. 22. Relationship between risk of overturning (D) and R_E

$$f = \frac{K_s}{I_r K_0} \tag{43}$$

and K_s is defined as

$$K_s = \frac{q_y}{s_s} \tag{44}$$

In this, r_s' becomes an important factor for D_{OT} when f is greater than 1.

Application of Risk Evaluation for Overturning

The relationship between the characteristics of ground penetration by the outrigger and I_r was investigated using the results of the centrifuge test. The index of brittle failure in the bearing ground (R_E) is defined as

$$R_E = \frac{K_0}{K_y} \tag{45}$$

where K_y=tangent modulus relative to q and s after yield.

Fig. 21 shows the relationship between R_E and I_r as obtained from the centrifuge test. For simplicity, K_y for both CT1 and CT9 were given by the tangent modulus at s/D=0.30 as the relationship between q and s was approximated by a hyperbola model. I_r indicates a tendency to decrease linearly to R_E as represented by a common logarithm when R_E is greater than 20, and the relationship between I_r and R_E is approximated by

$$I_r = a \log R_E + b \tag{46}$$

in which a and b are both coefficients of an arbitrary value. Values of a=−0.31 and b=1.43 were obtained from the centrifuge test. It is considered that both a and b depend on the kind and size of the mobile crane, as well as on the ground condition. Numerical calculation was carried out so as to investigate the influence of K_0, K_y, and the damping coefficient (C) on I_r. A1, A2, B1, and B2 from Fig. 21 indicate the results of the numerical calculation where an arbitrary K_0, K_y, and C were given in a bilinear model. The result of numerical calculation is similar to that for the centrifuge test as I_r decreases to R_E. It was confirmed, however, that differences in K_0, K_y, and C affect both the value of R_E which corresponds to the start of I_r decrease and the decrement rate for I_r.

The risk of overturning (D_{OT}) of an actual mobile crane with a hook load capacity of 200 kN was calculated using the analytical results from the centrifuge test. It is assumed that r_s' is greater than r_p, where both $I_r<1$ and $K_s=K_0$. Accordingly, D is derived as

$$D_{OT} = r_s' = f r_p = \frac{r_p}{-0.31 \log R_E + 1.43} \tag{47}$$

Fig. 22 shows the relationship between D_{OT} and R_E. In cases where $q_a=2/3q_y$ and $r_p=2/3$, D_{OT} exceeds 1 and the mobile crane overturns when R_E is greater than 300. Meanwhile, when $r_p=1/3$, D_{OT} is less than 1.0 for almost the entire range of R_E. In such a case, mobile cranes remain in a safe condition without any ground penetration by the outriggers.

A countermeasure to prevent overturning is needed when D_{OT} is greater than 1. Installing steel plates under the outriggers to increase the acting area, thereby decreasing the pressure acting on the ground, is one of these countermeasures. As a result of this modification, D_{OT} falls below 1.0 due to the decrease in r_p. It is also recommended that additional limitation be applied to the net rated load given in the current safety regulations. The acting pressure of the outriggers is reduced due to the decrease in hook load, and r_p falls below 1. Overturning as a result of ground penetration by the outriggers is prevented by introducing countermeasures commensurate with risk.

Conclusions

This study examines instability in mobile cranes caused as a result of ground penetration by the outriggers. Theoretical, experimental, and numerical analyses were carried out in order to clarify the effect of outrigger ground penetration on overturning. The conclusions of this study are summarized as follows.

1. The bearing capacity of layered ground with a hard surface overlaying soft ground is higher than that of uniform soft ground. However, the velocity of penetration into layered ground is higher than that of uniform soft ground. Mobile cranes become highly unstable as a result of rapid penetration of the outriggers. Consequently, it is important to evaluate the risk of overturning not only in terms of the bearing capacity of the ground, but also with regard to the penetration velocity caused by brittle failure of the bearing ground.

J. Constr. Eng. Manage., 2005, 131(6): 689-704

2. Centrifuge testing was performed in order to investigate the influence of the characteristics of ground penetration by the outriggers on overturning. Theoretical analysis of the equilibrium was carried out to allow introduction of both the static tilt angle (θ_s) and the dynamic tilt angle (θ_d) of the mobile cranes. Back-analysis using test records was carried out to confirm the kinetic tilt angle (θ_r) of actual kinetic equilibrium in testing. It was confirmed that θ_s and θ_d indicate the upper and lower limits of the equilibrium, respectively. θ_r approached θ_s when the velocity of ground penetration was lower due to ductile failure of the bearing ground. Meanwhile, θ_r approached θ_d when the velocity was higher due to the brittle failure of the bearing ground. Rapid ground penetration of the outriggers due to brittle failure made the mobile crane much more unstable.
3. An index of relative instability (I_r) was introduced as a way of studying the influence of factors such as the crane status, the moment, and the ground conditions for overturning. I_r is the ratio of ground penetration by the outriggers at static equilibrium (s_s) to that at kinetic equilibrium (s_r). Variations in both the crane status and the moment condition had little effect on I_r. However, an increase in the velocity of ground penetration reduced I_r. It was, therefore, ascertained that the velocity of ground penetration resulting from failure characteristics of the bearing ground had a major influence on the instability of the crane.
4. Numerical analysis was carried out to verify both the results of centrifuge testing and the influence of characteristics of the ground's bearing capacity. Both a hyperbola model and a bilinear model were used to approximate the relationship between the acting pressure on the outriggers (q) and the ground penetration ratio of the outriggers (s/D). The behavior of overturning and the analytical equilibrium generally coincided with the results of centrifuge test, although a slight difference in correspondence was seen in these cases. An accurate approximation of the relationships of $q-s/D$ and damping coefficient at ground penetration is needed for precise calculation of overturning.
5. The index of brittle failure for the bearing ground (R_E) was defined with reference to the results for the relationship between q and s/D in the centrifuge test, and the relationship between R_E and I_r was also investigated. The value of I_r decreased to that of R_E given by the common logarithm where R_E was greater than 20.
6. A risk evaluation method is proposed for overturning in mobile cranes and this utilizes the maximum values for failure risk of the bearing ground (r_p) and the kinetic risk due to ground penetration (r_s'). Both r_p and r_s' can be estimated using an on-site plate loading test. The potential for overturning exists when the risk of overturning (D_{OT}) is greater than 1, and countermeasures such as installing steel plates or decreasing the net rated load are needed to prevent overturning.
7. The value of the safety factor for bearing capacity of ground (F_s) is considered to be inverse to r_p. When information given by ground survey is limited to the ultimate bearing capacity (q_y), analytical results indicate that 3 is an appropriate value for F_s so as to maintain D_{OT} below 1. The value of F_s may be reduced to 1.5 in consideration of r_s' when R_E is obtained in addition to q_y.
8. A basic risk evaluation method is proposed using the determined value for both r_p and r_s' at present. However, the variables given by both ground survey and the crane status indicate distribution due to the corresponding uncertainties. Accordingly, reliability analysis in consideration of probability distribution would be needed to clarify D in further study.

References

Beliveau, Y., Dixit, S., and Dal, T. (1993). "Dynamic damping of payload motion for cranes." *J. Constr. Eng. Manage.,* 119(3), 631–644.

Bernold, L. E., Lorenc, S. J., and Luces, E. (1997). "Intelligent technology for truck crane accident prevention." *J. Constr. Eng. Manage.* 123(3), 276–284.

British Standards Institution (BSI). (1991a). "Code of practice for safe use of crane, Part 2: Inspection, testing and examination." *BS 7121*, 3–6.

British Standards Institution (BSI). (1991b). "Code of practice for safe use of crane, Part 2: Inspection, testing and examination." *BS 7121*, 13–14.

British Standards Institution (BSI). (2000). "Code of practice for safe use of crane, Part 3: Mobile crane." *BS 7121*, 14–16.

Cook, R. D., Malkus, D. S., and Plesha, M. E. (1989). "Concept and applications of finite element analysis," 3rd Ed., Wiley, New York, 408–409.

Finnie, I. M. S. (1993). "Performance of shallow foundations in calcareous soil." Dissertation, Doctor of Philosophy, Univ. of Western Australia.

Hambly, E. C. (1990). "Overturning instability." *J. Geotech. Eng.*, 116(4), 704–709.

Hambly, E. C. (1985). "Punch-through instability of jack-up on seabed." *J. Geotech. Eng.,* 111(5), 545–550.

Ingram, W. B., and Dutt, R. N. (1987). "Discussion of 'Punching through instability of jack up on seabed' by E. C. Hambly." *J. Geotech. Eng.*, 113(4), pp. 402–403.

International Organization for Standardization (ISO). (1991). "Mobile cranes, determination of stability." *ISO 4305*, 1–3, Genova, Switzerland.

Ito, H. (1994). "General statement of mobile crane." *Kajima shuppan-kai*, 47–49 (in Japanese), Minato-ku, Tokyo, Japan.

Japan Crane Association (JCA). (1998). "Japanese legislation for cranes and mobile cranes." 30, 138, and 139, Shinagawa-ku, Tokyo, Japan.

Japan Crane Association (JCA). (2002). "A year book of crane in 1994 edition." 39 (in Japanese), Shingawa-ku, Tokyo, Japan.

Labour Standard Bureau, Ministry of Labour, Japan. (1978). "Writ of Ministry of Labour No.45." *Ordinance on Safety of Crane and Similar Equipment* (in Japanese), Chiyoda-ku, Tokyo, Japan.

Maeda, Y., and Inoue, I. (1973). "Physical modeling of the dynamic limiting equilibrium." *Journal of Japan Society for Safety Engineering*, 12(3), 198–202 (in Japanese).

Rajagopalan, K. S. (1988). "Supports for traveling cranes: Case history." *J. Constr. Eng. Manage.,* 114(1), 114–120.

Standards Association of Australia (SAA). (1993a). "Cranes-safe use, Part 1: General requirements." *AS2550.1-1993*, 9 and 32, Homebush, New South Wales, Australia.

Standards Association of Australia (SAA). (1993b). "Cranes-safe use, Part 5: Mobile and vehicle-loading cranes." *AS2550.5-1993*, 4 and 5, Homebush, New South Wales, Australia.

Standards Association of Australia (SAA). (1995). "Cranes (including hoist and winches), Part 5: Mobile and vehicle-loading cranes." *AS1418.5-1995*, 8–23, Homebush, New South Wales, Australia.

Tamate, S., Horii, N., Toyosawa, Y., Suemasa, N., and Takano, Y. (1998a). "Instability of mobile cranes due to penetration of outriggers." *J. Geotech. Eng.*, 596/3–43, 163–174 (in Japanese).

Tamate, S., Horii, N., Toyosawa, Y., Suemasa, N., and Takano, Y. (1998b). "Simulating the overturning of mobile cranes due to penetration of outriggers." *Proc., Centrifuge 98*, 901–906.

U.S. Department of Labor, Occupational Safety and Health Administration. (1994). "Mobile crane inspection guidelines for OSHA compli-

J. Constr. Eng. Manage., 2005, 131(6): 689-704

ance officers, Chapter 2: Mobile cranes, Section 2.1: Lifting principles." ⟨http://www.osha.gov/SLTC/cranehoistsafety/mobilecrane/mobilecrane.html⟩ (Aug. 22, 2003).

U.S. Department of Labor, Occupational Safety and Health Administration. (2000). "Part 1910—Occupational safety and health standards, subpart N—Material handling and storage, 1910.180—Crawler, locomotive and truck crane." ⟨http://www.osha.gov/pls/oshaweb/owadisp.show_document?p_table=STANDARDS&p_id=9831⟩ (Aug. 22, 2003).

Zaretsky, A. A., and Shapiro, H. I. (1997). "Overturning stability of a free standing crane under dynamic loading." *SAE Technical Paper Series*, Society of Automotive Engineers, No. 972721, 1–9, United States.